Journal of Sound and Vibration (2000) **238**(1), 171–178
doi:10.1006/jsvi.2000.3013, available online at http://www.idealibrary.com on IDEAL®

LETTERS TO THE EDITOR

CHANGING THE PROPAGATION DIRECTION OF FLEXURAL ULTRASONIC PROGRESSIVE WAVES BY MODULATING EXCITATION FREQUENCY

B.-G. Loh and P. I. Ro

Precision Engineering Center, North Carolina State University, Raleigh, NC, U.S.A.

(*Received* 12 *July* 1999, *and in final form* 24 *February* 2000)

1. INTRODUCTION

When flexural waves propagate, particles on the surface of the vibrating beam move elliptically. Then, an object on the beam is forced to move in the opposite direction of wave propagation through frictional force [1]. Changing wave propagation directions reverse transport direction of an object. In references [2, 3], the change in wave propagation direction was made possible connecting either a voltage source or absorptive circuitry to either active or passive modules. In reference [4], modulating the relationship between phase differences in excitation forces allows for alteration of wave propagation direction. However, in reference [5], it was observed that changing the excitation frequency also caused the direction of wave propagation to reverse. This particular phenomenon has never been observed. Also, the dependency of the wave propagation direction on the excitation frequency has important ramifications on the active control of object transport using ultrasonic flexural progressive waves. This paper presents changing the wave propagation direction of flexural ultrasonic progressive waves with variations in the excitation frequency.

2. PROTOTYPE AND WORKING PRINCIPLES

The prototype in Figure 1 consists of a beam and modules that contain piezoelectric actuators and horns [6]. The beam and horns are made of 6061-T6 aluminum because of the excellent acoustical characteristics of this material. The beam is 11 mm wide, 3·1 mm thick and 500 mm long. The piezoelectric actuators are bolted Langevin-type transducers (BLT) manufactured by NGK Spark Plug Co. Ltd. (model no. DA2228). Their resonant frequency is 28 kHz. As shown in Figure 2, two sets of identical horn-and-actuator modules were assembled with each of the supporting structures. The horns were attached to the supporting structure at the nodes of the horns. Each set was designed to operate independently.

The two modules are supplied with sinusoidal voltages of the same frequency but with a phase difference of 90°. Using normal mode expansion, the vibration of the beam can be represented by the linear superposition of an infinite number of natural mode shapes of vibration [7, 8]. Of particular interest are the two modes that have natural frequencies closest to the excitation frequency. The vibration amplitudes of these two modes are large, compared to other mode shapes. Therefore, the vibration can be approximated by

0022-460X/00/460171 + 08 $35.00/0

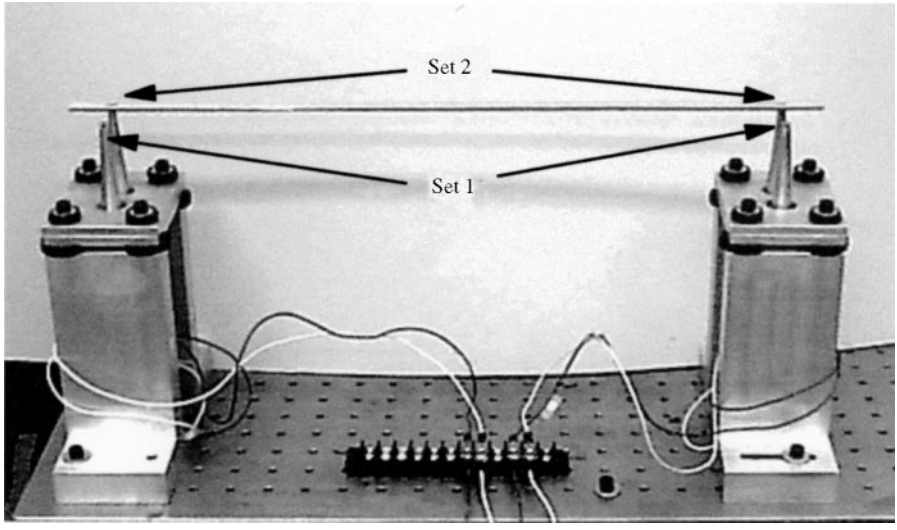

Figure 1. Prototype.

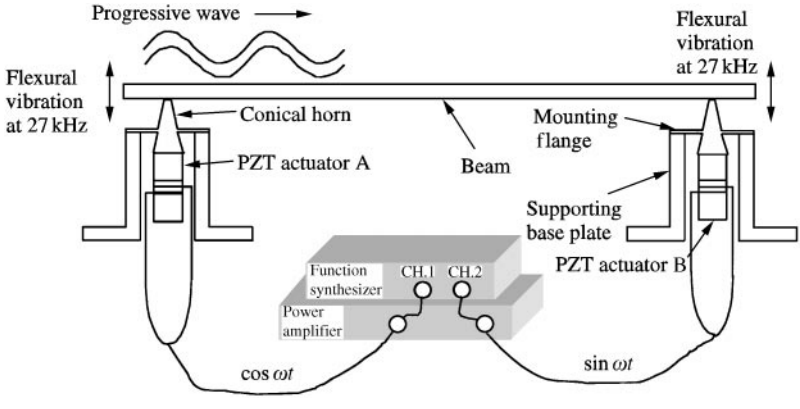

Figure 2. Schematic drawing of prototype.

a superposition of these two mode shapes. Excitation of these two modes with the same frequency but a phase difference of 90° generates progressive waves for a finite beam length [4]. Effective excitation of the two neighboring mode shapes is critical for generating progressive waves. If the beam is connected with the horns at the node of any mode shapes of the beam, those mode shapes are not excited. The degree to which a mode is excited increases as the excitation location approaches the anti node of the mode. Therefore, the beam was connected at the anti nodes of two mode shapes whose natural frequencies are closest to the excitation frequency. With the excitation frequency of 27 kHz, those locations are 27 mm from the ends of the beam.

3. MODELLING

The prototype is modelled as a beam excited with forces that have the same frequency but a phase difference of 90°. As shown in Figure 3, l_1 and l_2 are the distances to the locations

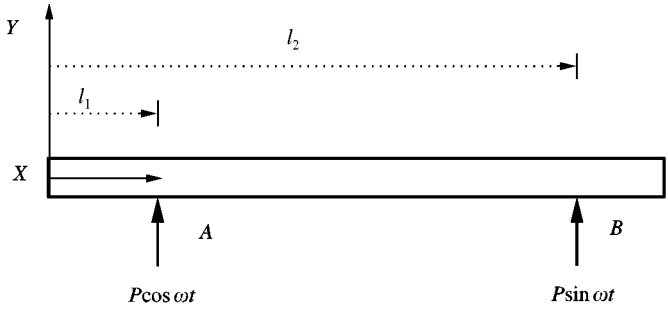

Figure 3. Beam model of prototype.

where the beam is connected with the horns, ω is the excitation frequency, and P is the peak amplitude of the force.

The steady state flexural vibration of the beam can be expressed using normal mode expansion:

$$y(x, t) = P\cos\omega t \sum_{n=1}^{\infty} \frac{\Phi_n(x)\Phi_n(l_1)}{\omega_n^2 - \omega^2} + P\sin\omega t \sum_{n=1}^{\infty} \frac{\Phi_n(x)\Phi_n(l_2)}{\omega_n^2 - \omega^2}, \tag{1}$$

where ω_n is a natural frequency of the beam and $\Phi_n(x)$ is a normalized mode shape. The vibration $y(x, t)$ is a linear superposition of an infinite number of mode shapes. The contribution that a mode makes to the total vibration depends upon the location of the applied force and the proximity of its natural frequency to the excitation frequency. Accordingly, the major contribution to the total vibration stems from the mode shapes whose natural frequencies are closest to the excitation frequency. Since this study is intended to verify reversal of the wave propagation direction as a function of the excitation frequency, the vibration can be approximated by the mode shapes making major contribution. Mode shapes are defined as [8]

$$\phi_n(x) = \sin\beta_n x + \sinh\beta_n x + \alpha(\cos\beta_n x + \cosh\beta_n x), \tag{2}$$

where β_n is the wave number defined as $\beta_n = 2\pi/\lambda_n = \omega_n^{1/2}(\rho a/EI)^{1/4}$, λ the wave length, ρ the mass density of the beam, a the cross-sectional area, E the Young's modulus, I the cross sectional area of moment, α the $(\sin\beta_n l - \sinh\beta_n l)/(\cos\beta_n l - \cosh\beta_n l)$.

As the mode number grows, α approaches -1 and $\sinh\beta_n x - \cosh\beta_n x \cong 0$. Thus, equation (2) can be approximated as

$$\phi_n(x) = \sqrt{2}\sin(\beta_n x - \pi/4). \tag{3}$$

When the excitation frequency is chosen to mostly excite the 30th and 31st modes of the beam, the flexural vibration as shown in equation (1) can be approximated as

$$y(x, t) = \{C_1\sin(\beta_{30}x - \pi/4)\cos(\omega t) + C_2\sin(\beta_{31}x - \pi/4)\sin(\omega t)\}$$
$$+ \{C_3\sin(\beta_{31}x - \pi/4)\cos(\omega t) + C_4\sin(\beta_{30}x - \pi/4)\sin(\omega t)\}, \tag{4}$$

TABLE 1

Measured and estimated natural frequency

	Resonant frequency, (kHz)		
	Measured	Estimated	
		B–E	Timoshenko
1	20·7	20·1	20·6
2	22·5	21·6	22·1
3	23·6	23·3	23·6
4	24·9	24·9	25·1
5	26·1	26·6	26·7
6	27·1	28·4	28·3
7	28·1	30·2	30·0
8	29·7		

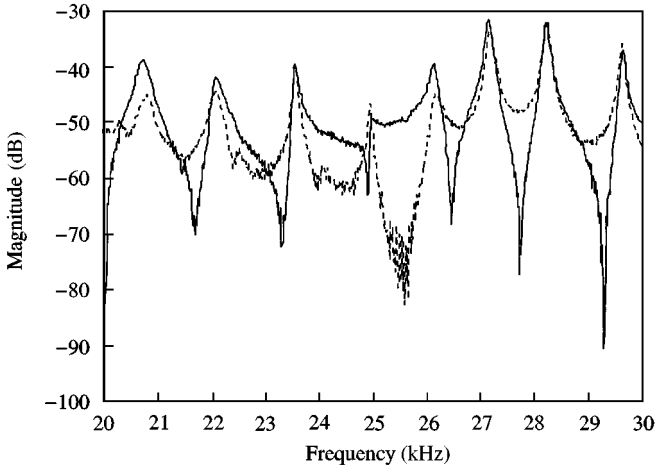

Figure 4. Frequency spectrum of the system: ——, collocated measurement; – – –, non-collocated measurement.

where C_n, $n = 1, \ldots, 4$, are constants defined as

$$C_1 = \frac{2P\Phi_{30}(l_1)}{(\omega_{30}^2 - \omega^2)\sqrt{\rho a}}, \qquad C_2 = \frac{2P\Phi_{31}(l_2)}{(\omega_{31}^2 - \omega^2)\sqrt{\rho a}},$$

$$C_3 = \frac{2P\Phi_{31}(l_1)}{(\omega_{31}^2 - \omega^2)\sqrt{\rho a}}, \qquad C_4 = \frac{2P\Phi_{30}(l_2)}{(\omega_{30}^2 - \omega^2)\sqrt{\rho a}}. \tag{5}$$

The first curly bracket of $y(x, t)$ in equation (4) represents one progressive wave while the second curly bracket represents another. The direction of wave propagation is determined by the signs of the constants, C_n, that are a function of the excitation frequency, ω, as shown in equation (5). In Table 1, the measured natural frequencies obtained from the frequency spectrum in Figure 4 are compared with the estimated natural frequencies using Bernoulli–Euler (B–E) beam theory and Timoshenko beam theory respectively. The

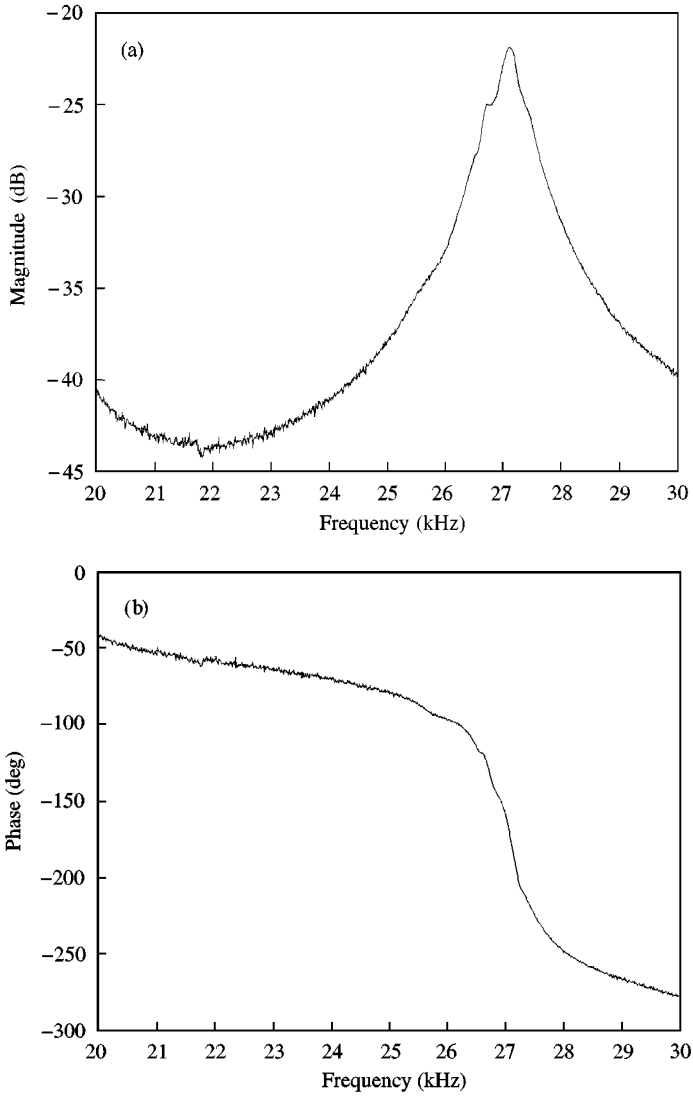

Figure 5. Frequency spectrum of BLT: (a) magnitude, (b) phase.

resonant frequency obtained by B–E beam theory corresponds well to those obtained by Timoshenko beam theory because the beam is thin and long, thereby, shear force and rotary inertia do not play as much of a role as bending moment and transverse inertia in determining resonant frequency. The measured natural frequencies agree well with the estimated ones except that the estimation has one more resonant frequency. This additional resonant frequency stems from the BLT designed to resonate at 28 kHz. When it was assembled with the horn and the supporting structure, due to the mass loading effect, its resonant frequency was shifted to 27·2 kHz. The frequency spectrum of the BLT is shown in Figure 5, which clearly shows a resonance at 27·2 kHz. This additional resonance arising from the BLT when attached to the beam should be considered as one of the natural frequencies of the system for the following analysis.

TABLE 2

Wave propagation direction with respect to the signs of the constants C_n

C_1	C_2		C_3	C_4	
+	+	A ← B	+	+	A → B
+	−	A → B	+	−	A ← B
−	+	A → B	−	+	A ← B
−	−	A ← B	−	−	A → B

TABLE 3

Wave propagation direction with respect to excitation frequency

k	ω_k (kHz)	ω_{k+1} (kHz)	ω (kHz)	C_1	C_2	Wave propagation direction based on C_1 & C_2	C_3	C_4	Wave propagation direction based on C_3 & C_4
25	18·6	20·1	19·4	+	+	⇐	−	+	⇐
26	20·1	21·6	20·9	+	−	⇒	−	−	⇒
27	21·6	23·3	22·5	+	+	⇐	−	+	⇐
28	23·3	24·9	24·1	+	−	⇒	−	−	⇒
29	24·9	26·6	25·8	+	+	⇐	−	+	⇐
30	26·6	27·1	26·9	+	−	⇒	−	−	⇒
31	27·1	28·4	27·8	+	+	⇐	−	+	⇐
32	28·4	30·2	29·3	+	−	⇒	−	−	⇒
33	30·2	32·1	31·2	+	+	⇐	−	+	⇐
34	32·1	34·1	33·1	+	−	⇒	−	−	⇒
35	34·1	36·1	35·1	+	+	⇐	−	+	⇐

To observe the relationship between the direction of wave propagation and the sign of C_n in equation (5), the wave propagation direction was simulated using Matlab. The results are shown in Table 2. When C_1 and C_2 have the same signs, the waves propagate from B to A in Figure 3. When C_3 and C_4 have the same signs, the waves propagate from A to B. When two progressive waves travel in opposite directions, the resultant wave propagates in the same direction as the wave with a bigger amplitude. Observing the signs of C_n and the amplitudes of two progressive waves represented in curly brackets in equation (4) enables the estimation of the propagation direction with variations in the excitation frequency. Table 3 and Figure 6 shows the change in the direction of wave propagation with respect to the excitation frequency. When $k = 25$, the excitation frequency is chosen to be an average of natural frequencies (19·4 kHz) associated with the 25th and 26th modes. As a result, the response is dominated by those modes. It is noted that as k increases the constants C_2 and C_4 alternate their sign, resulting in a change in wave propagation direction.

To test the change in the wave propagation direction, an object weighting 30 g was placed on the beam and the speed was measured using an infrared sensor. The results are shown in Figure 7. At an excitation frequency below 27·1 kHz, the 30th and 31st modes have the greatest excitation. The wave propagation direction was observed from A to B. At an excitation frequency above 27·1 kHz, the 31st and the 32nd become the modes with the greatest excitation, resulting in a reversal of the wave propagation direction. These results coincide with the results presented in Table 3. When $k = 30$, the wave propagated from A to B. The wave propagation direction is reversed when $k = 31$.

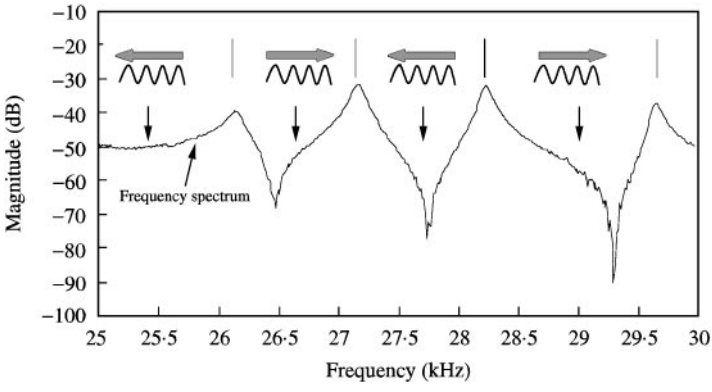

Figure 6. Change of wave propagation direction with respect to excitation frequency. ⟷ wave propagation direction; ↓ location of excitation frequency.

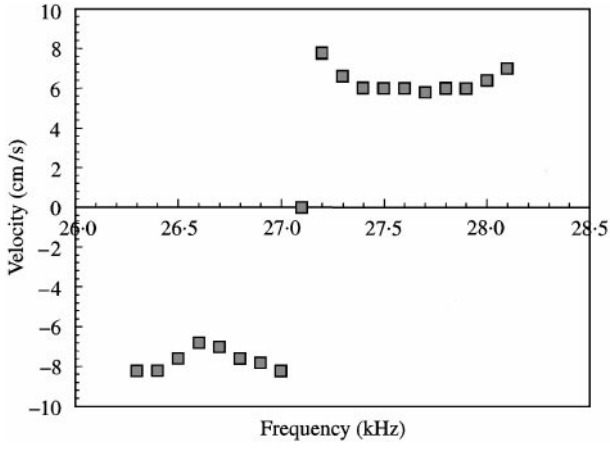

Figure 7. Experimental results of change of wave propagation direction.

4. CONCLUSIONS

Based on the frequency spectrum of the prototype system, the resonance of the system due to the resonance of the transducer was observed. This is crucial in estimating the response of the system because of its location with regard to the excitation frequency. This resonance is included as one of the natural frequencies of the system in the model derived using Bernoulli–Euler beam theory, which clearly explains the change in wave propagation direction. In literature, it has been reported that 90° out-of-phase excitation of two consecutive modes of the beam generates a travelling wave on the beam surface and that the wave propagation direction in reversed by the changing phase relationship between excitation forces. In this work, it was shown that changing the direction of wave propagation is also made possible by modulating excitation frequency without changing the phase relationship between excitation forces. When the excitation frequency is increased such that the next two consecutive modes are most excited, the waves reverse the propagation direction. This process continues as the excitation frequency increases. The simulations showed clear changes in the direction of the wave propagation at an excitation

frequency of 27·1 kHz. The simulation results were in good agreement with the experimental results.

REFERENCES

1. S. Ueha, Y. Tomikawa, M. Kurosawa and N. Nakamura 1993 *Ultrasonic Motors*, 9–17. Oxford: Claredon Press.
2. M. Kuribayashi, S. Ueha and E. Mori 1989 *Journal of Acoustical Society of America* **77**, 1431–1435. Excitation conditions for flexural traveling waves for a reversible ultrasonic linear motor.
3. M. Kurasawa and S. Ueha 1989 *Ultrasonics* **27**, 39–44. High speed ultrasonic linear motor with high transmission efficiency.
4. Yoshiro Tomikawa, Kazunari Adachi, Hiroshi Hirata, Takanori Suzuki and Takehiro Takano 1989 *Proceedings of* 10*th Symposium on Ultrasonic Electronics*, Vol. **29-1**, 179–181. Excitation of progressive wave in a flexurally vibrating transmission medium.
5. Byoung-Gook Loh and Paul I. Ro 1999 *IEEE Transaction on Ultrasonic, Ferroelectrics, and Frequency Control*. An object transport system using flexural ultrasonic progressive waves generated by two-mode excitation (in press).
6. L. G. Merkulov 1957 *Soviet Physics Acoustics* **3**, 246–255. Design of ultrasonic concentrators.
7. M. P. Norton 1989 *Fundamentals of Noise and Vibration Analysis for Engineers* 94. Cambridge: Cambridge University Press.
8. Singiresu S. Rao 1995 *Mechanical Vibrations*, 527. MA, Addison-Wesley.